Proton-Conducting Dense Ceramic Membranes for Hydrogen Separation

Technical Report

(Final)

10/01/00

09/31/04

Jerry Y.S. Lin
Vineet Gupta
Scott Cheng

November 2004

DE-FG26-00NT40818

Department of Chemical and Materials Engineering
University of Cincinnati
Cincinnati, OH 45221-0171

DISCLAIMER

ABSTRACT

Dense thin films of $SrCe_{0.95}Tm_{0.05}O_{3-\delta}$ (SCTm) with perovskite structure were prepared on porous alumina or SCTm substrates by the methods of (1) polymeric-gel casting and (2) dry-pressing. The polymeric-gel casting method includes preparation of mixed metal oxide gel and coating of the gel on a macroporous alumina support. Micrometer thick SCTm films of the perovskite structure can be obtained by the polymeric-gel casting method. However, the deposited films are not hermetic and it may require about 50 coatings in order to obtain gas-tight SCTm films by this method. Pd-Cu thin films were synthesized with elemental palladium and copper targets by the sequential R.F. sputter deposition on porous substrates. Pd-Cu alloy films could be formed after proper annealing. The deposited Pd-Cu films were gas-tight. This result demonstrated the feasibility of obtaining an ultrathin SCTm film by the sequential sputter deposition of Sr, Ce and Tm metals followed by proper annealing and oxidation. Such ultrathin SCTm membranes will offer sufficiently high hydrogen permeance for practical applications.

Thin gas-tight SCTm membranes were synthesized on porous SCTm supports by the dry-pressing method. In this method, the green powder of SCTm was prepared by wet chemical method using metal nitrates as the precursors. Particle size of the powder was revealed to be a vital factor in determining the porosity and shrinkage of the sintered disks. Small particle size formed the dense film while large particle size produced porous substrates. The SCTm film thickness was varied from 1 mm to 0.15 mm by varying the amount of the target powder. A close match between the shrinkage of the substrate and the dense film led to the defect free-thin films. The selectivity of H_2 over He with these films was infinite. The chemical environment on each side of the membrane influenced the H_2 permeation flux as it had concurrent effects on the driving force and electronic/ionic conductivities. The H_2 permeation rates were found to be inversely proportional to the thickness of the dense film indicating that bulk diffusion rather than surface reaction played a dominant role in H_2 transport through these dense films within the studied thickness range (150 μm – 1 mm).

TABLE OF CONTENTS

INTRODUCTION

Dense proton-conducting ceramic membranes have received increasing interest since Iwahara and coworkers first discovered proton-conduction in $SrCeO_3$ based perovskite type ceramics at high temperatures (>500ºC) in a hydrogen-containing atmosphere [1]. One of the major driving forces for this increasing interest is the need for larger amount of pure H_2, which is a clean energy fuel for transportation section. Dense thin-ceramic membranes fabricated from mixed electronic/protonic conductors at high temperatures provide a simple and efficient means for separating H_2 from coal-derived syngas. H_2 separation is achieved in a non-galvanic mode, without the need for an external power supply and hence offers economic advantage over existing technologies [2].

The two most extensively studied high temperature proton-conducting ceramics (with the highest proton conductivity) are $SrCe_{O.95}Yb_{0.05}O_3$ (SCYb) and $BaCe_{0.9}Nd_{0.1}O_3$ (BCNd). Under pure H_2, at 900°C, proton conductivities of SCYb and BCNd are about $0.7xl0^{-2}$ and $2.2xl0^{-2}$ S/cm, respectively. Although both SCYb and BCNd contain considerable amounts of O^{2-} vacancy, SCYb is essentially a non-oxygen ionic conductor but BCNd shows O_2 ionic conductivity in the same order of magnitude as its proton conductivity at temperature higher than 800°C [11, 12]. Therefore, BCNd is not suitable for applications in membrane reactors for partial oxidative dehydrogenation reaction or as electrolytes in fuel cells for electric power generation. $SrCeO_3$ based ceramics exhibit much lower O_2 ionic conductivity.

In general, both protonic and electronic conductivities determine the H_2 permeation flux through proton-conducting membranes. The major problem with the $SrCeO_3$ based ceramic membranes is their low electronic conductivity that leads to low H_2 permeability. Low H_2 permeation flux was reported for $SrCe_{O.95}Yb_{0.05}O_3$ (SCYb) membranes with no O_2 in the sweep gas due to its low electronic conductivity under non-oxidative atmosphere [3]. An effective way to improve the H_2 permeability of $SrCeO_3$ based proton-conducting ceramic membranes is to improve their electronic conductivity. It can be achieved either by doping aliovalent ions in Ce^{3+} site or by adding metal phase (10-40 vol. %) to proton conducting ceramic powders [4-6].

Effect of different dopants on electronic conductivity of these protonic conductors has been studied extensively by many researchers [7-10]. According to the hopping mechanism of electronic conduction in oxide ceramics [11], the electronic conductivity is inversely related to the ionization potential of Ce and dopants. Qi and Lin [9] have selected thulium (Tm) as the dopant for preparing the modified $SrCeO_3$ membranes with improved electronic conductivity. Due to the low fourth ionization energy of Tm (23.7ev), the $SrCe_{0.95}Tm_{0.03}O_3$ (SCTm) membrane exhibits a high proton conductivity of 10^{-2} S/cm in H_2 at 900°C, which is comparable to SCYb. H_2 permeation experiments using the SCTm membrane of thickness 2 mm showed a high H_2 permeation flux of 5.0×10^{-7} mol/cm^2·s at 900°C, under upstream and downstream H_2 partial pressure of 0.l atm and 10^{-6}atm, respectively [9]. However, the thick (l-2mm) SCTm membrane still do not offer sufficiently high H_2 permeance as compared to metal membranes in the temperature range of 500-700°C for many membrane reactor applications.

Recently, Hamakawa et. al. [12] spin-coated $SrCe_{0.95}Yb_{0.05}O_3$ (SCYb) slurry on a porous $SrCeO_3$ support. The H_2 permeation flux of 2.0 μm thick membrane was reported to be 1.2×10^{-6} mol/cm^2.s. The H_2 permeation flux was found to be inversely proportional to the thickness of the dense layer even for 2 μm SCYb films. However, the synthetic process is rather laborious and sensitive. It is difficult to fabricate the thin films in large scale with this synthetic procedure. Xia and Liu [13, 14] introduced dry pressing to fabricate dense ceramic electrolyte layers on porous

substrates. This method appears simple and cost-effective for synthesis of thin supported mixed-conducting ceramic membranes for gas separation.

The objective of this project was to prepare thin proton-conducting ceramic membranes by different methods and to study hydrogen permeation properties of these thin membranes. A dry-press method was developed to prepare thin thulium doped $SrCeO_3$ membranes of various thicknesses. Both dense layer and porous layer in SCTm asymmetrical membranes were obtained by carefully controlling the particle size of powders and other process variables. The thickness of dense layer was controlled by the amount of powder in the dense layer. H_2 permeation properties of these proton-conducting ceramic membranes were studied under different chemical environment, membrane thickness and temperature to find the optimum operating conditions. Research was also conducted to explore polymer-gel coating and sputter deposition methods to prepare thin proton-conducting inorganic membranes.

EXECUTIVE SUMMARY

Tm doped $SrCeO_3$ (SCTm) was found to be the best protonic/electronic perovskite-type ceramic conductor in our lab. Several methods were studied for preparation of thin SCTm membranes. We were successful in preparing dense-thin films of SCTm down to thickness 150 μm by using simple and cost effective approach of dry pressing. Membrane thickness was varied from 1 mm to 150 μm by adding the controlled amount of SCTm powder uniformly on the surface of the support layer. The $SrCe_{0.95}Tm_{0.05}O_3$ powder was prepared by citrate method from metal nitrates. Particle size of the powder was found to be the vital factor in determining the porosity and gas tightness effect of sintered disks. Small particle size formed dense film while large particle size produced porous substrate. Thickness of the dense layer can be further reduced by optimizing the particle size of the powders.

The H_2 permeation of these membranes was studied at high temperatures (750-900 ^oC) in a high temperature permeation system. Membranes were sealed with the alumina tube of the permeation system using a ceramic sealant of composition 45% $SrCe_{0.95}Tb_{0.05}O_3$, 50% Pyrex glass, and 5% $NaAlO_2$. H_2 permeation fluxes were obtained under wide range of operating conditions such as membrane thickness, temperature, upstream H_2 partial pressure and downstream O_2 partial pressure. It was found that the H_2 permeation flux increases on reducing the thickness of the dense films, indicating that the bulk diffusion rather than the surface reaction played a dominant role in the H_2 transport within the studied thickness range (3- 0.15 mm). It seems very likely because the surface dissociation of H_2 molecules requires lower energy as compared to O_2. H_2 permeation flux of 9.37×10^{-8} mol/cm^2·s was obtained at 900 ºC with a 150 μm thick SCTm membrane when 10% H_2/He and air were used as feed gas and sweeping gas respectively. In order to reach the level of commercial interests, the hydrogen permeation flux should be at least 7.4×10^{-7} mol/cm^2·s. Therefore, by extrapolation of linear inverse relationship between hydrogen flux and membrane dense layer thickness, the membrane thickness should be at least reduced to 15 μm.

The activation energy for H_2 permeation through the SCTm membrane is about 116 kJ/mol in 600-700 ºC and 16 kJ/mol in 750-950 ºC. This indicates a change in the electrical and protonic conduction mechanism at around 700 ºC. The H_2 flux increases with increasing downstream O_2 partial pressure for all the membrane thicknesses studied in O_2 partial pressure range of 0.1 atm to 1.0 atm. No hydrogen flux was detected (detection limit 10^{-9} mol/cm^2.s) when only N_2 was used as a sweep gas. Feed gas used in these conditions was 10% H_2/He. This

indicates that the hole conductivity part of the total electrical conductivity controls the H_2 permeation flux under conditions where one side of the membrane is exposed to oxidizing condition (O_2/N_2 or partial pressure of $O_2 > 10^{-5}$ atm) and the other side is exposed to reducing condition (H_2/He or partial pressure of $O_2 < 10^{-20}$ atm).

Micrometer thick SCTm films of the perovskite structure can be obtained by a polymeric-gel casting method. However, the deposited films are not hermetic and it may require about 50 coatings in order to obtain gas-tight SCTm films by this method. The feasibility of making ultrathin SCTm film was demonstrated using sequential R.F. Sputter deposition of elemental Pd and Cu targets. Pd-Cu alloy films could be formed on porous substrates after proper annealing. The ratio of the concentration of Cu to the concentration of Pd in the deposited layer increases on increasing the ratio of the deposition times for Cu and Pd though the increment in the ratio of concentrations of deposited metals is not proportional to the ratio of their corresponding deposited time. This indicates that the composition of the final Pd-Cu film can be controlled by the deposition time. This result demonstrated the feasibility of obtaining an ultrathin SCTm film by the sequential sputter deposition of Sr, Ce and Tm metals followed by proper annealing and oxidation. Such ultrathin SCTm membranes will offer sufficiently high H_2 permeance for practical applications.

EXPERIMENTAL

Thin Membranes Prepared by Polymer-Gel and Sputter Deposition Approaches

Sr-Ce-Tm containing inorganic-organic polymeric sol was prepared from $Sr(NO3)2$, $Ce(NO3)_3$ and $Tm(NO3)_3$ in stoichiometric proportions (100-Sr, 95-Ce. 5-Tm) (for 0.02 mole SCTm) in 20 ml distilled water, followed by mixing with 10 ml concentrated nitric acid, 40 ml ethylene glycol and 3 g glycine. The nitric acid and glycine was used to adjust and stabilize the pH value in the reacting solution. The solution was then heated to 93-96^{o}C and stirred for 60 h at this temperature till the viscosity of the solution was in the range of 90~190 cP at room temperature. A highly viscous polymeric gel containing Sr, Ce and Tm in the desired proportion was obtained.

Submicron-pore α-alumina disks were dip-coated with the viscous polymeric gel (contact time 10-15 min), followed by drying at 40^{o}C for 2 h. The dip-coated polymer gels were calcined at 300^{o}C in air for 3.5 h, and the supported disks were dip-coated again with the polymer gel, followed by the same drying and calcination step, to obtain thicker SCTm layers. The final coated layers were sintered 1500°C for 13 h to convert the coated SCTm layers into the perovskite structure and to densify the coated layers. The membranes were characterized by XRD for phase structure and membrane thickness (confirmed by SEM), and helium permeation for gas tightness.

To test feasibility of depositing multi-metal oxide films on porous substrate using pure metals as the targets, Pd-Cu films were prepared on composite ceramic supports. These supports consist of a porous α-alumina disks coated with γ-alumina on one side. The porous α-alumina disks (2.0 mm thick and 0.2 μm average pore diameter) were prepared by pressing α-alumina powder (Alcoa) with a mechanical press at a pressure of 10 MPa followed by sintering at 1150 °C for 30 h. The membranes were deposited by RF magnetron sputtering using a plasma sciences CRC-150 dc/rf magnetron-sputtering unit. Pure copper and palladium foils, 0.1 mm in thickness, were the elemental targets. Before each run the sputtering chamber was evacuated down to the

pressure in the range of 10^{-6} Torr for a period of 2 h and then back filled with UHP argon at a pressure of 5×10^{-3} Torr. The deposition procedure was repeated with switched targets. The multilayer membranes were then annealed in a temperature programmable tubular furnace. The system was heated up to 500–600ºC at a ramp of 120 ºC/h. The purpose of changing the annealing conditions was to optimize this process with respect to the temperature, time and atmosphere.

Proton-Conducting Ceramic Membrane Synthesis by Dry Pressing Method

The citrate method was used to prepare the perovskite-type $SrCe_{0.95}Tm_{0.05}O_3$ powder. $Sr(NO_3)_2$, $Ce(NO_3)_3.6H_2O$ and $Tm(NO_3)_3.5H_2O$ were mixed in stoichiometric proportions with citric acid in distilled water to form a 0.2 M solution of total metal ions. The molar amount of the citric acid was 1.5 times higher than the total molar amount of the metal ions. This solution was heated to 96 ºC–100 ºC for 5 h with stirring in a refluxed mode, where polymerization reaction took place. The water was evaporated and the solution was condensed to a sticky gel. After drying at 110 ^oC for 24 h, the gel-like material became a sponge-like and brittle material. It was self-ignited at 400 ^oC for 30 min. The material after self-ignition was ground to powder with a mortar and pestle for about 10 min and calcined at 600 ºC for 10 h to remove the residual organic compounds.

The raw powder was pressed roughly at a pressure of 5 MPa with a hydraulic press in a die of diameter 25 mm to form the thick, porous support layer. Another part of the raw powder was carefully ground in an agate mortar for about 15 min. A controlled amount of this powder was added uniformly on the surface of the support layer in the die holder. The two-layer sample in the die holder was pressed again at a final pressure of 130 MPa and finally co-sintered at 1495 ^oC for 24 h with a heating and cooling rate of 120 ^oC/h.

Membrane Characterization

The gas tightness of the membranes was checked by helium permeation method. High temperature hydrogen permeation for SCTm membranes was conducted on a high-temperature permeation setup installed in our lab. The sealant was composed of 45% SCTb powder, 50% pyrex glass and 5% $NaAlO_2$. The sealant powder in desired composition was grinded in an agate mortar for several minutes to form a sticky paste. The sticky paste was then put on the top of the inner dense alumina tube (25.4 mm in OD, from Coors Ceramics). The asymmetrical membrane disk of diameter 21 mm was put onto the paste. The surface of dense layer of this asymmetrical membrane should be in contact with the paste in order to get complete sealing effect. For metal membranes, the thickness of the deposited film was determined from X-ray diffraction (XRD) pattern. XRD analysis of membranes was carried out with a Siemens Kristalloflex D500 diffractometer, with Cu Kα radiation and 2θ changed from 20 to 70^0. The composition of Cu in Pd-Cu was calculated using the relationship between the d-space and the concentration of metal alloys [15].

RESULTS AND DISCUSSION

Membranes Prepared by Polymeric Gel Coating Method

The critical parameter for coating a continuous SCTm film on porous alumina substrates by this method is the viscosity of gel. It was found that the viscosity of 109 cp is optimum for dip-coating. Figure 1 shows the XRD patterns of the uncoated α-alumina support (0 dip-coating) and the same support coated with SCTm layer of different dip-coating numbers (after sintering at 1400^{o}C). As shown, the coated SCTm layers have desired perovskite structure. Furthermore, the XRD peak intensity of the perovskite phase increases with increasing number of coating, consistent with the fact that multiple coating gives thicker SCTm layer. SCTm films up to 10 μm can be obtained through multiple coatings. Each coating gives a SCTm layer of about 1 μm in thickness.

Figure 2 shows helium permeance through the uncoated α-alumina support and the same support coated with SCTm layers. A straight line, characteristic of the combined Knudsen and viscous flow transport mechanism, can correlate the helium permeance data. Helium permeance decreases with increasing number of coating due to increased resistance as a result of thicker SCTm layer. The reduction in helium permeance is not significant even after 10 cycles of dip-coating. These data suggest that it is very difficult to obtain a hermetic SCTm layer by this method. A rough estimate indicates that repeated coating of SCTm for about 50 times would result in a fairly hermetic SCTm membrane with SCTm thickness of about 50μm.

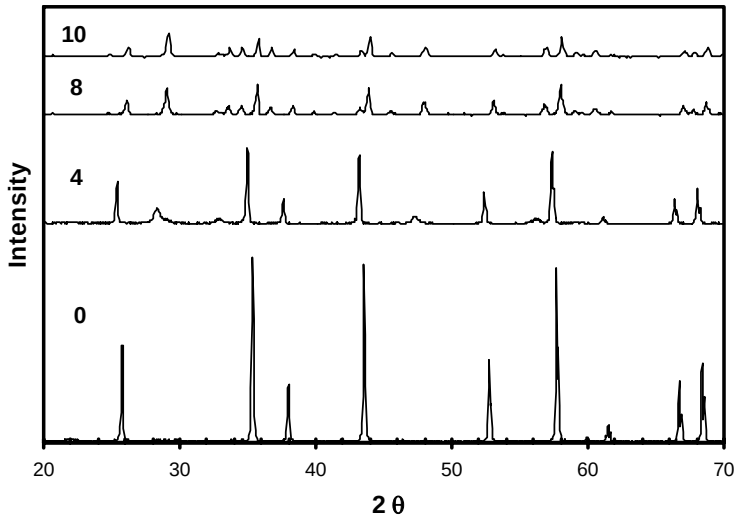

Figure 1 XRD Patterns of Alumina Supported SCTm Membranes Prepared by the Polymeric Gel Method with Different Number of Dip-Coating

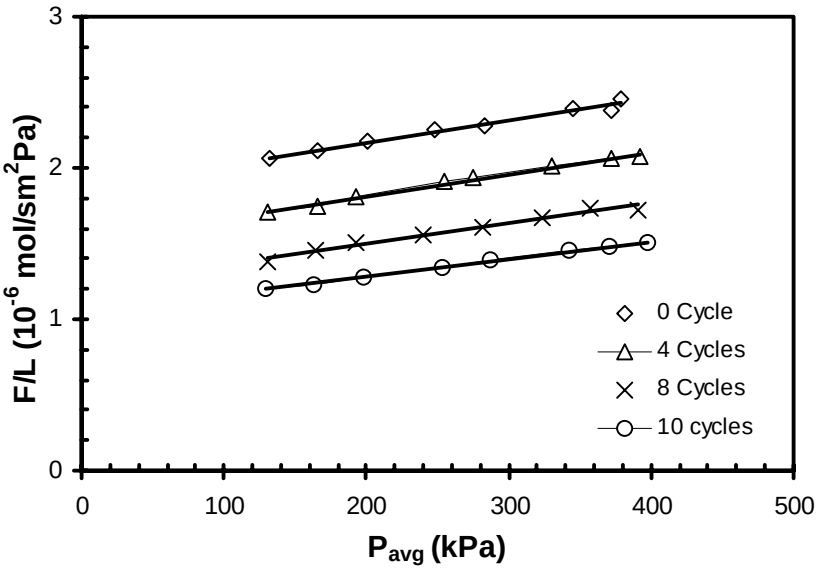

Figure 2 Helium Permeance versus Average Pressure across Membrane for of Alumina Supported SCTm Membranes Prepared by the Polymeric Gel Method with Different Number of Dip-Coating (Cycles)

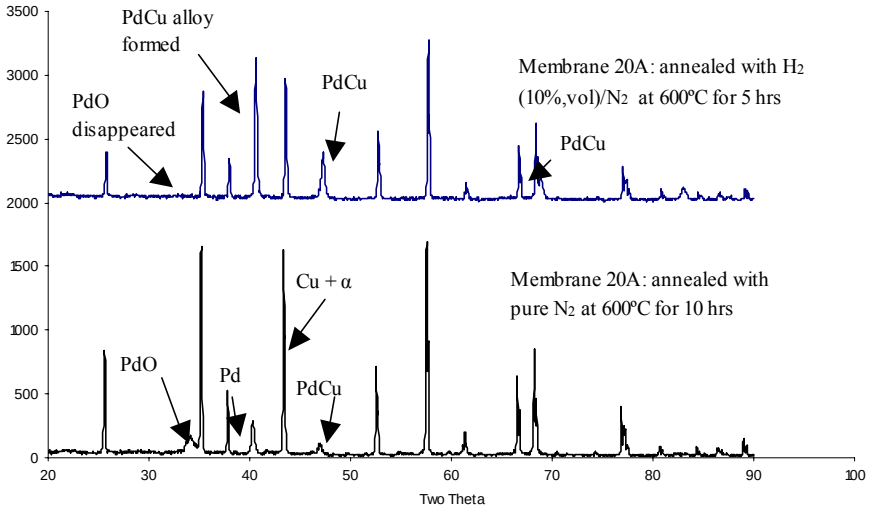

Figure 3 XRD patterns of membrane 20 after annealing under different atmospheres

Pd-Cu Membranes Prepared by Sputtering Deposition

Table 1 gives the synthetic process and the properties of several Pd-Cu membranes prepared with a sequential deposition method. Figure 3compares the XRD patterns of sample 20. XRD data indicates that the PdO phase was formed on the membrane sample when annealing was carried out in an atmosphere of pure nitrogen at high temperature (referred to as membrane 20A).

Formation of PdO can be explained by the fact that the remaining oxygen in the annealing system oxidized Pd at elevated temperature. Subsequently, when the same sample was annealed in the atmosphere of 10% H_2/N_2, the PdO peak in XRD pattern disappeared (referred to as membrane 20B in Figure 3), and an alloy of Pd-Cu is formed. This indicates that a reducing atmosphere is indispensable for the formation of Pd-Cu alloy. As summarized in Table 1, the ultrathin Pd-Cu membranes of thickness 70-120 nm can be obtained by the sequential sputter deposition method. The ratio of the concentration of Cu to the concentration of Pd in the deposited layer increases on increasing the ratio of the deposition times for Cu and Pd though the increment in the ratio of concentrations of deposited metals is not proportional to the ratio of their corresponding deposited time. This indicates that the composition of the final Pd-Cu film can be controlled by the deposition time. All the membranes listed in Table 1 are gas tight to helium. However, the membranes with lower Cu concentrations delaminated from the support after hydrogen permeation experiments. This can be attributed to the hydrogen embrittlement. The Pd-Cu membrane with higher Cu dopant (40%) remained intact on the support after hydrogen permeation measurements. This is because doping Cu, similarly to Ag, modifies the metal-hydride temperature two-phase diagram, suppressing hydrogen embrittlement.

Table 1 Analysis of the Composition of Pd-Cu Film Deposited by Sequential Sputtering Method

Sample	Total deposition time	Deposition interval time	Deposition time ratio [Cu/Pd]	Measured [Cu/Pd] ratio (or Cu%)	Thickness (nm)	Pd-Cu layer lamination situation
18	8 min Cu, 20 min Pd	Cu: 8 min Pd: 10 min	0.4	0.13 (11.9)	76	Delaminated after hydrogen permeation experiment
20	25 min Cu, 45 min Pd	Cu: 8 min Pd: 10 min	0.53	0.19 (16.2)	94.7	20% delaminated after hydrogen permeation experiment, but totally laminated after subsequent gas tightness
21	24 min Cu, 30 min Pd	Cu: 8 min Pd: 10 min	0.82	0.28 (22.4)	116.8	Remained intact after initial stage of hydrogen permeation experiment, laminated at higher concentration of H_2 (2 atm)
22	30 min Cu, 14 min Pd	Cu: 10 min Pd: 7 min	2	0.66 (40.7)	72.6	Remained intact after hydrogen permeation experiments at high pressure (2 atm, 250 °C)

Synthesis of Proton-Conducting Membranes by Dry Press Method

Preparation conditions and the properties of the representative SCTm samples were summarized in Tables 2 and 3. The average particle size of substrates PI to P6 is respectively 7 μm, 0.2 μm, 0.5 μm, 20 μm, 45 μm, 70 μm as determined form their SEM images. The gas

tightness of these membranes was checked with an unsteady state gas permeation system at room temperature. The % shrinkage of the disks was calculated by measuring the diameter of the disk before and after thermal treatment. From Table 2 it can be seen that samples 1, 5, and 8 are the potential candidates of porous substrates. It was noted that as the particle size increases, the % shrinkage of the membrane became smaller and the porosity became larger until it was laminated.

Table 2 SCTm symmetrical membranes prepared under various situations and their properties

Disk Sample No.	Ts[1]/time (ºC/hr)	SubstrateTc[2]/ time (ºC/hr)	Substrate	Gas Tight	Appearance of Sintered Disks	Shrinkage %	Good for H_2 Separation
# 1	1495(24)	600(10)	P1	No	Slight green dark	19	No
# 2	1260(24)	600(10)	P2	No	Slight yellow	5	No
# 3	1495(24)	600(10)	P2	Yes	Green dark	22	Yes
# 4	1495(24)	800(10)	P3	Yes	Green dark	21	Yes
# 5	1495(24)	1300(10)	P4	No	Slight green dark	15	No
# 6	1495(24)	1400(10)	P5	No	Partially laminated	11	No
# 7	1495(24)	1500(10)	P6	No	Totally laminated	8	No

[1] Ts stands for the final sintering temperature, [2]Tc stands for powder calcination temperature

Table 3 shows the SCTm asymmetrical membranes based on three potential candidates of porous substrates. Sample 9, and 11 were gas tight and could be served as good membranes for H_2 separation experiments. Sample 10, and 12 were still porous though their top layer particle size was same as sample 9. It could be due the larger difference in shrinkage rate between top layer and substrate. It was also observed that when the amount of powder P2 was reduced to 0.2 g, keeping all the conditions same as for disk 9, gas tight membranes could not be formed. It could be because too much of a thin layer could not stand interfacial resistant force caused by shrinkage difference between layers. The minimum thickness of dense film obtained by this approach is 150 μm. The thickness of dense layer could be directly calculated from the amount of powder and was also confirmed by optical microscopy. The representative photo was shown in Figure 3. The thickness of dense layer could be further reduced if particle size of top layer and substrate are further optimized.

The mixture of SCTm and α-alumina was also studied as the porous support. Although 0.4 g of P2 could not form dense film on the porous support of 20% α-alumina and 80% SCTm due to large difference in shrinkage rate, it seems exciting to see the sample 11 that consists of 0.2 g P2 could get gas tight on substrate of 10% α-alumina and PI. However, the XRD pattern of the support indicates that α-alumina and SCTm reacted each other. Al atoms may substitute Ce atoms, which could distort the perovskite structure. Hence, the representative peaks could not be clearly seen in the X ray diffraction pattern. From the appearance, one could see both top layer surface and support had changed into the reddish-yellow color. The alumina atoms probably

migrated into the top layer and created a different color. Sample #11 could not exhibit tangible H_2 permeation flux. It also confirms that some α-alumina diffused into SCTm.

Table 3 SCTm asymmetrical membranes prepared under various situations and their properties

Disk Sample No.	Ts[1]/time (ºC/hr)	SubstrateTc[2]/time (ºC/hr)	Top layer	Substrate	Gas Tight or Not	Appearance of Sintered Disks	Shrinkage Rate(%)	Good for H_2 Separation or Not
# 8	1495(24)	600(10)	0.6g P2	3.6g P1	Yes	Top side is darker than substrate side	19	Yes
# 9	1495(24)	1300	0.6g P2	3.6g P4	No	Slight green dark	15	No
[1] Ts stands for the final sintering temperature, [2]Tc stands for powder calcination temperature								

The typical light microscopy image of asymmetrical SCTm membrane is shown in Figure 4. This image clearly shows that the cross section is divided into two layers. The top layer appears to be dense while the bottom layer looks porous. However, this appearance could not be found in the image of sample # 11. The homogenous cross section of sample #11 support the assumption of atomic migration.

Hydrogen Permeation Model Development

H_2 permeation through dense proton-conducting ceramic membranes was modeled based on the ambipolar diffusion theory by considering three moving charged species: proton, electron and electronic hole. The modeling results in a general flux equation from which explicit equations for hydrogen permeation flux can be derived for proton-conducting ceramic membranes operated in hydrogen separation and membrane reactor modes. The final expressions relate hydrogen permeation flux to the experimentally measurable variables including membrane thickness, upstream and downstream hydrogen partial pressures, and temperature. The parameters in these hydrogen permeation flux expressions include electron, hole or proton conductivity or concentration at a reference state (P_{H2}=1 atm) with explicit physical meaning, which can be regressed from the experimental hydrogen permeation data or obtained by independently designed measurement.

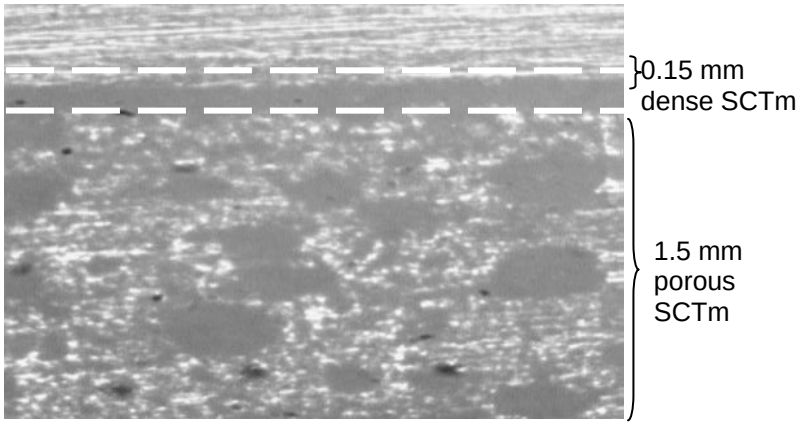

Figure 4 Light Microscopic Image of SCTm Membrane

For hydrogen permeation through proton-conducting ceramic membranes with proton transference number closed to one, the model gives the following hydrogen permeation flux equation:

$$J_{H_2} = \frac{RT}{2LF^2}(\sigma_e^o P_{H_2}^{'1/2} + \sigma_h^o P_{H_2}^{''-1/2}) \quad (1)$$

where σ_h^o and σ_e^o are the electronic-hole and electron conductivity at P_{H2}= 1 atm, P'_{H2} and P''_{H2} are the hydrogen partial pressure in the upstream and downstream of the membranes. It should be noted that in this case the hydrogen partial pressure P''_{H2} can not be measured directly because air is present at the downstream side. P''_{H} in Eq. (1) should be calculated from the experimentally measurable oxygen and water vapor partial pressures in the downstream side using a thermodynamic equilibrium relationship. Eq. (1) shows that the hydrogen permeation flux increases with increasing upstream pressure and decreasing downstream pressure. σ_h^o is usually very small. However, the equilibrium P''_{H2} in air-water mixture is also very small. As a result, the second term in Eq. (1) can be very significant.

Hydrogen Permeation Experimental Results

The hydrogen permeation flux, J_{H_2} (mol/m^2.s) was calculated from the following equation:

$$J_{H_2} = \frac{P_{sat}}{RT}(\Delta RH)Q_{downstrean}\frac{1}{A} \quad (2)$$

Here $Q_{downstream}$ (mol/m^3) is the total flow rate of the sweep gas stream, ΔRH is the difference in the relative humidity at the outlet and the inlet of the sweep gas , A (m^2) is the cross-sectional area of the membrane, and P_{sat} (N/m^2) is the saturated vapor pressure of the air at temperature T (K). The upstream equilibrium hydrogen partial pressure was obtained as:

$$P_{H_2}^{''} = \frac{K_w P_{H_2O}}{P_{O_2}^{''1/2}} \quad (3)$$

Here K_w is the thermodynamic equilibrium constant of the water dissociation reaction as shown below:

$$H_2O \Leftrightarrow H_2 + \frac{1}{2}O_2 \quad (A)$$

The hydrogen permeation flux was measured by changing different parameters such as membrane thickness, temperature, upstream H_2 partial pressure, and downstream O_2 partial pressures. Steady state permeation data were acquired after 1 h of changing the operating conditions.

Figure 5 shows the influence of downstream O_2 partial pressure on the H_2 permeation flux at 900 ^oC for SCTm membranes of different thickness. The H_2 flux increases with increasing downstream O_2 partial pressure at O_2 pressure range of 0.1 to 1.0atm. The upstream side was exposed to 10% H_2/He. No H_2 flux ($<10^{-9}$ mol/cm^2/s based on the sensitivity of the permeation apparatus) was observed when only He ($p_{o2} = 1\times10^{-5}$) was used as sweep gas. Figure 6 shows the influence of upstream H_2 partial pressure on the H_2 permeation flux at 900^{o}C. The downstream side of the membrane was exposed to 20% O_2/N_2. One could see that the H_2 flux increased with the upstream H_2 partial pressure.

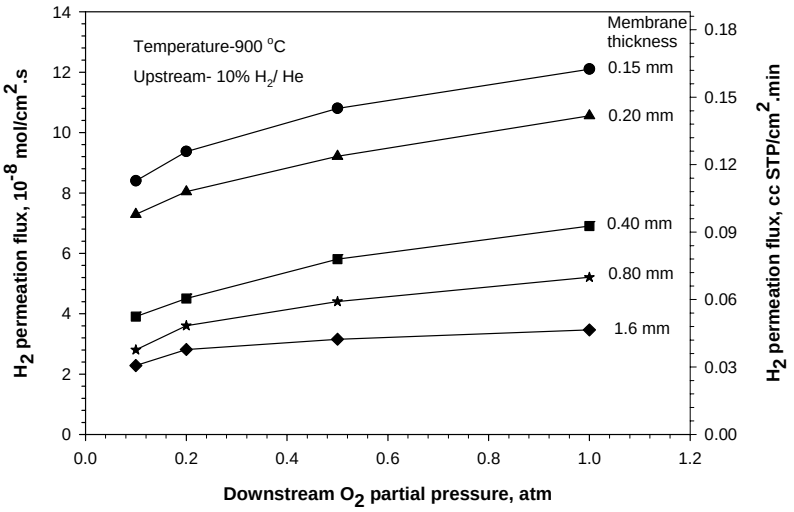

Figure 5 Influence of Downstream Oxygen Partial Pressure on the H_2 Permeation Flux of SCTm Membranes

These results indicate that the hydrogen permeation rates are influenced by the atmosphere on both sides of the SCTm membrane. These effects can be explained by considering the effects of chemical environment on the total driving force and the concentrations of electrons, holes and protons. Generally the H_2 permeation flux across a ionic conducting membrane is described by the Wagner equation that assumes the bulk diffusion is the rate limiting step:

$$J_{H_2} = \frac{RT}{4F^2L}\int_{p'_{H_2}}^{p''_{H_2}} \frac{\sigma_{OH^\bullet}(\sigma_{h^\bullet} + \sigma_{e'})}{\sigma_t} d\ln P_{H_2} \qquad (4)$$

The charge carrier concentrations are related to the gaseous H_2 and O_2 partial pressure by the following equilibrium reactions:

$$\frac{1}{2}O_2 + V_O^{\bullet\bullet} \Leftrightarrow O_o^x + 2h^\bullet \qquad (B)$$

$$H_2 + 2O_O^x \Leftrightarrow 2OH^\bullet + 2e' \qquad (C)$$

From reaction (B) and (C) one can see that at the feed side (10 % H_2/He) of the membrane, reaction (C) shifts to the right and reaction (B) shifts to the left because of very low level of oxygen partial pressure (10^{-18} -10^{-33} atm) making electrons as the major carrier for electronic conduction on the feed side of the membrane. On the downstream side holes are the major electronic carrier due to the higher partial pressures of the O_2 ($p_{O2} > 10^{-5}$ pressure on the feed side will membrane. It also increases the net driving force for hydrogen permeation resulting in net increase in the H_2 permeation flux as observed in Figure 6.

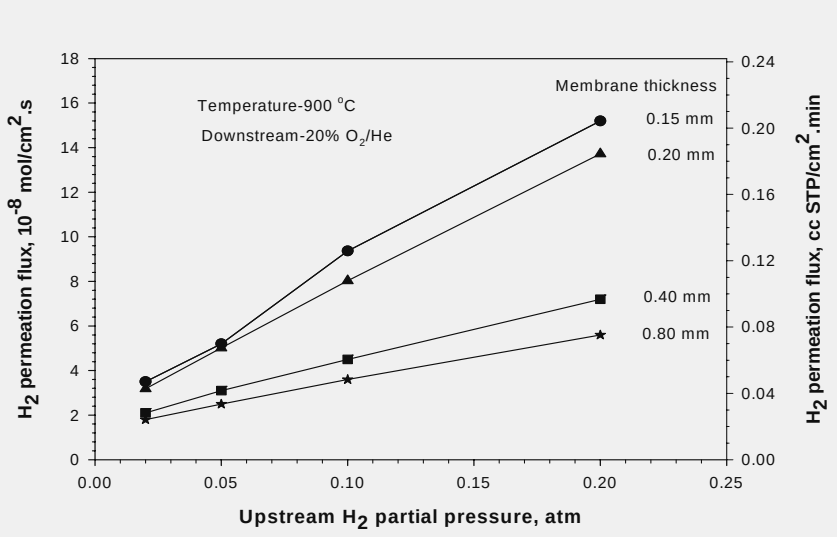

Figure 6 Influence of Upstream H_2 Partial Pressure on the H_2 Permeation Flux of SCTm Membrane

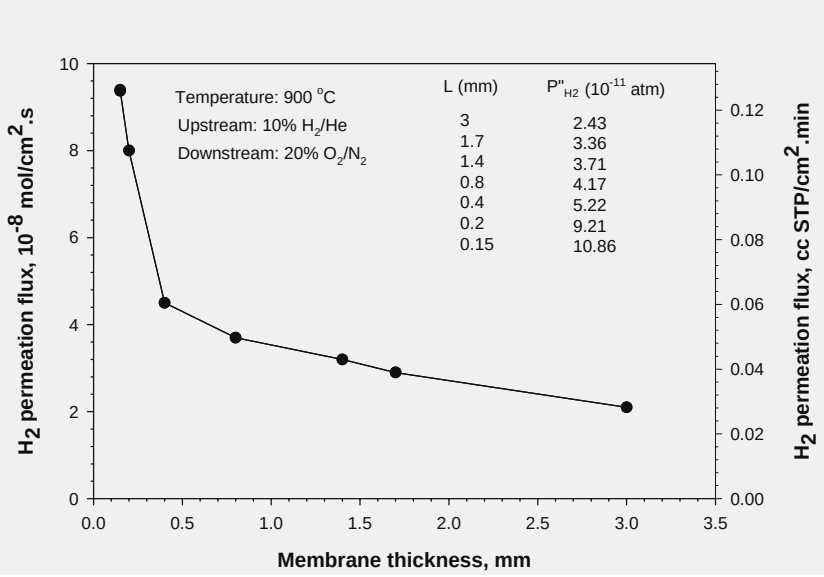

Figure 7 H_2 permeation flux versus membrane thickness

Increasing O_2 partial pressure on the downstream side of the membrane increases the hole concentration and hence their conductivity in the membrane. The higher downstream O_2 partial pressure would have a lower H_2 equilibrium partial pressure that creates a higher driving force for H_2 permeation. The combination of these two effects results in increase in the hydrogen flux on increasing O_2 partial pressure in the feed side. When only N_2 ($p_{O2} \sim 10^{-5}$ atm) was present in the downstream side no H_2 permeation was observed indicating n-type conduction is very negligible through the membrane under these operating conditions. The same permeation behavior was observed in $SrCe_{0.95}Yb_{0.05}O_3$.

Figure 7 plots H_2 flux versus thickness of dense layer in the range of 3 to 0.15 mm. It can be seen from the figure that the hydrogen permeation flux increases with decreasing the membrane thickness. This indicates that the bulk diffusion step is important for H_2 transport through SCTm membrane in the studied thickness range (3-0.15 mm). It should be noted that

there would be an increase in the downstream H_2 partial pressure as the membrane thinner due to increasing H_2 permeation flux. Thus, the driving force for H_2 permeation through thinner membrane is smaller than the thicker ones. Considering this effect one might not expect a linear relationship between hydrogen flux and reciprocal of the membrane thickness even though bulk diffisuion is rate limiting. The H_2 flux versus temperature data were regressed by the Arrhenius equation. Activation energy of H_2 diffusion in SCTm membranes could be estimated based on the relationship between the hydrogen permeation flux and temperature.

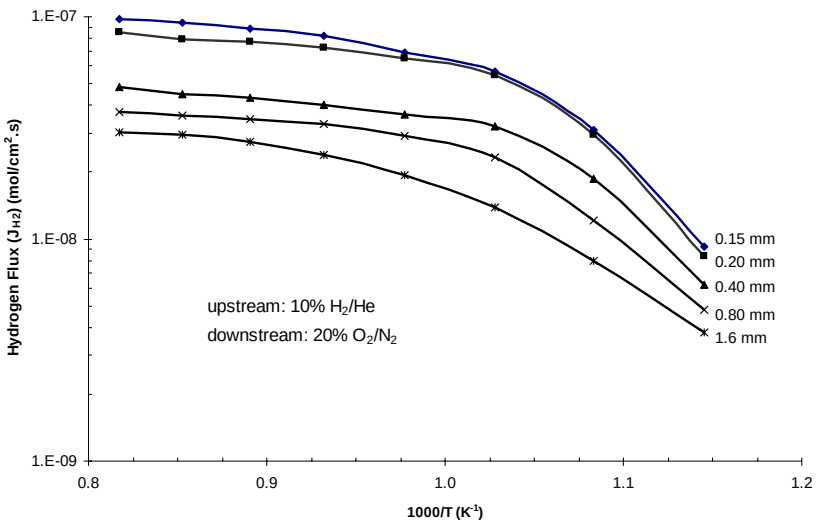

Figure 8 Temperature Dependence of Hydrogen Permeation Flux of SCTm Membranes

Figure 8 plots the natural logarithm of hydrogen flux against the reciprocal of temperature for the SCTm membranes of various thicknesses at a fixed upstream H_2 partial pressure. Each curve in Figure 8 can be divided into two straight lines with different slopes in a lower temperature region (≤700 °C) and a high temperature region (700-950 °C). The activation energy calculated from the slopes of these lines are given in Tables 4 and 5. It shows that the activation energy at low temperature region (in Table 4) is much higher than the activation energy at high temperature region (in Table 5). This indicates a change in electrical and protonic conduction mechanism at around 700 °C. It should be noted that downstream hydrogen partial pressure increases with increasing temperature at a given upstream partial pressure. Therefore, the activation energy estimated should be considered as an average value.

Table 4 Activation Energies and Preexponential Constant for SCT Membrane in 600-700 ºC

Membrane thickness (mm)	0.15	0.2	0.4	0.8	1.6	Average value
Activation energy E (kJ/mol)	129.3	132.9	116.5	111.5	91.3	116.3
Preexponential constant K^0 (mol/cm^2.s)	5.43×10^{-1}	8.12×10^{-1}	6.24×10^{-2}	2.32×10^{-2}	1.11×10^{-3}	2.9×10^{-1}

Table 5 Activation Energies and Preexponential Constants for SCTm Membrane in 750-950 ºC

Membrane thickness (mm)	0.15	0.2	0.4	0.8	1.6	Average value
Activation energy E (kJ/mol)	17.46	13.09	13.97	12.32	23.35	16.04
Preexponential constant K^0 ($mol/cm^2.s$)	5.57×10^{-7}	3.09×10^{-7}	1.90×10^{-7}	1.28×10^{-7}	3.17×10^{-7}	3.00×10^{-7}

CONCLUSIONS

Micrometer thick SCTm films of the perovskite structure can be obtained by the polymer-gel coating method. However, the deposited films are not hermetic and it may require about 50 coatings in order to obtain gas-tight SCTm films by this method. The synthetic procedure of Pd-Cu alloy was established with sputtering deposition system by sequential deposition of the individual elemental targets. The resulting Pd-Cu films are alloy, ultrathin and gas-tight to helium. These results demonstrate the potential to make ultrathin SCTm membranes by the sequential sputter deposition of Sr, Ce, and Tm followed by oxidation under controlled conditions.

Dry pressing approach proved to be effective for the preparation of SCTm pervoskite asymmetrical membrane disks. Particle size was found to be the key factor in determining the porosity of layers in final membrane disks. The interfacial resistance force caused by the difference of shrinkage between layers affects the gas-tightness of top layer. There is a compromise between the particle size and difference in shrinkage to fabricate a good asymmetrical membrane. The thinnest dense layer achieved in this work is 150 μm. This thickness could be reduced further when particle size is optimized with respect to porosity and shrinkage difference between the layers. A H_2 permeation flux of 9.37×10^{-8} $mol/cm^2 \cdot s$ was obtained at 900ºC with a 150 μm thick SCTm membrane when 10% H_2/He and air were used as feed gas and sweeping gas, respectively. The H_2 permeation flux of SCTm is comparable with one of the best studied proton-conducting ceramic membranes, $SrCe_{0.95}Yb_{0.05}O_{3-\delta}$. The H_2 flux increased with increasing the downstream side O_2 partial pressure indicating that hole conductivity controlled the H_2 permeation flux. H_2 permeation rates increased on reducing the thickness of the dense layers suggesting that the bulk diffusion in SCTm membrane is the rate-limiting step at the studied thickness range (3-0.15 mm).

Meanwhile, these H_2 permeation data provide a good source for understanding of mixed ionic/electronic transport through the membrane. Based on the inverse relation between the membrane thickness and the hydrogen permeation flux, we can extrapolate that the hydrogen flux of value as high as $3x10^{-6}$ $mol/cm^2.s$ (or 4 $cc/cm^2.min$) could be obtained for the SCTm membrane that is 5 μm thick at 900°C. The synthetic procedure of Pd-Cu alloy was established with sputtering deposition system by sequential deposition of the individual elemental targets. The resulting Pd-Cu films are alloy, ultrathin and gas-tight to helium. These results demonstrate the potential to make ultrathin SCTm membranes by the sequential sputter deposition of Sr, Ce, and Tm followed by oxidation under controlled conditions.

REFRENCES

1) F. S. Galasso, Structure, Properties and Preparation of Perovskite-Type Compounds, Pergamon Press, 13 (1969)
2) U. Balachandran, J. Guan, S. E. Dorris, Development of proton-conducting membranes for hydrogen separation, Paper presented at the Advanced Coal-Based Power and Environmental Systems 98 conference, Morgantown, WV July 21-23, (1998)
3) S. Humakawa, T. Hibino, H. Iwahara, Electrochemical hydrogen permeation in a proton-hole mixed conductor and its application to a membrane reactor, Journal of the Electrochemical Society, 14,1720 (1994)
4) S. E. Dorris, T. H. Lee, U. Balachandran, Metal/ceramic composites with higher hydrogen permeability, US patent 656926, 2003, to the University of Chicago (IL)
5) E. D. Wachsman, J. Naixiong, Two-phase hydrogen permeation membrane, US patent 6235417, 2001, to Her Majesty the Queen in the right of Canada, as represented by the Minister of (Ottawa, CA)
6) M. Mundschau, V. Michael, Hydrogen transport membranes, WO03076050, 2003, to Eltron Research Inc.
7) S.-J. Song, E. D. Wachsman, S. E. Dorris, U. Balachandran, Defect structure and n-type electrical properties of $SrCe_{0.95}Eu_{0.05}O_{3-\delta}$, J. Electrochemical Society, 150, A1484 (2003)
8) T. K. Shimura, Esaka, H. Matsumoto, H. Iwahara, Protonic conduction in Rh-doped $AZrO_3$ (A=Ba, Sr, and Ca), Solid State Ionics, 149, 237 (2002)
9) X. W. Qi, Y.S. Lin, Electrical conduction and hydrogen permeation through mixed proton-electron conducting strontium cerate membranes, Solid State Ionics, 130: (1-2) 149 (2000)
10) X. W. Qi, Y.S. Lin, Electric conducting properties of terbium doped strontium cerate, Solid State Ionics, 120, 85 (1999)
11) W. D. Kingery, H. K. Bowen, D. R. Uhlmal, Introduction to Ceramics, Wiley, New York, p.866 (1976)
12) S. Hamakawa, L. Lin, A. Li, E. Iglesia, Synthesis and hydrogen permeation properties of membranes based on dense $SrCe_{0.95}$ $Y_{0.05}O_3$ thin films, Solid State Ionics, 48, 71 (2002)
13) C. Xia, M. Liu, A simple and cost-effective approach to fabrication of dense ceramic membranes on porous substrates, Journal of American Ceramic Society, 84 [8] 1903 (2001)
14) C. Xia, M. Liu, Low-temperature SOFCs based on $GdO_{0.1}Ce_{O.90}O_{1.95}$ fabricated by dry pressing, Solid State Ionics, 144, 249 (2001)
15) C. S. Barrett, T. B. Massalski, Structure of metals: crystallographic methods, principles and data, 3rd ed., Oxford, New York: Paragon (1980)